COMMUNICATIONS PHYSICS

ARTICLE

DOI: 10.1038/s42005-018-0076-6 OPEN

# Atomic imprinting into metallic glasses

Rui Li[1], Zheng Chen[1], Amit Datye[1], Georg H. Simon[1,3], Jittisa Ketkaew[1], Emily Kinser[1], Ze Liu[1,4], Chao Zhou[1], Omur E. Dagdeviren[1], Sungwoo Sohn[1], Jonathan P. Singer[2,5], Chinedum O. Osuji[2], Jan Schroers[1] & Udo D. Schwarz[1,2]

Nanoimprinting by thermoplastic forming has attracted significant attention due to its promise of low-cost fabrication of functionalized surfaces and nanostructured devices, and metallic glasses have been identified as a material class ideally suited for nanoimprinting. In particular, their featureless atomic structure suggests that there may not be an intrinsic size limit to the material's ability to replicate a mould. Here we demonstrate atomic-scale imprinting into a platinum-based metallic glass alloy under ambient conditions using atomic step edges of a strontium titanate single crystal as a mould. The moulded metallic glass replicates the 'atomic smoothness' of the strontium titanate, with identical roughness to the one measured on the mould even after multiple usages and with replicas exhibiting an exceptional long-term stability of years. By providing a practical, reusable, and potentially high-throughput approach for atomic imprinting, our findings may open novel applications in surface functionalization through topographical structuring.

[1] Department of Mechanical Engineering and Materials Science, Yale University, New Haven, CT 06511, USA. [2] Department of Chemical and Environmental Engineering, Yale University, New Haven, CT 06511, USA. [3] Present address: Department of Chemical Physics, Fritz Haber Institute of the Max Planck Society, 14195 Berlin, Germany. [4] Present address: Department of Engineering Mechanics, School of Civil Engineering, Wuhan University, Wuhan, Hubei 430072, China. [5] Present address: Department of Mechanical and Aerospace Engineering, Rutgers University, Piscataway, NJ 08854, USA. These authors contributed equally: Rui Li, Zheng Chen. Correspondence and requests for materials should be addressed to U.D.S. (email: udo.schwarz@yale.edu)

The relative ease and speed at which large surface areas can be functionalized through structural patterning has been a major driver for developing imprinting methods and materials that can yield small features over large area substrates[1–3]. Typically, imprinting involves the embossing of a hard mould into a soft material. Due to the convenient adjustability of their degree of softening, thermoplastic polymers had been the material class of choice for most imprint procedures[4–6], but metallic glasses have recently gained popularity since they combine favourable mechanical and electrical properties[7–9]. The decisive factor for a material to qualify for moulding is its flowability, which is inversely proportional to its (apparent) viscosity[10]. Microscopically, the flow related to the pressing-into-form process is achieved through a shear movement of the flow units of the material, which can be grains in granular material and chains in polymers[11]. With decreasing mould feature size, the flow unit dimension may become comparable with the mould feature, which results in a sharp increase in flow resistance that prohibits the creation of structures smaller in scale than the flow unit's diameter[12].

Liquids may feature atoms or molecules as flow units, but the dominance of capillary forces over viscous ones counteracts a controlled filling of small spaces, making them challenging to be used for small-scale moulding[12,13]. When using molten metals, surface reactivity may in addition lead to the formation of contaminant layers such as oxides. As a result, liquid metals have thus far not been employed for nanometre-scale moulding. Both impediments can, however, be eliminated when using appropriate bulk metallic glasses (BMGs). These materials are vitrified metallic liquids whose robustness against crystallization gives convenient access to viscosities that are ideal for thermoplastic forming when heated above their glass transition temperature $T_g$[9,12–14].

Limited by mould size constraints, features as small as 13 nm have been demonstrated with BMGs via thermoplastic forming[12]. Assuming that atoms are indeed the flow units in BMGs, one could speculate that ultimately, atomic-scale features can be achieved[13]. However, it has long been postulated that plastic deformation may not occur atom-by-atom, but collectively in so-called shear-transformation zones (STZs)[13,15,16], with experimental evidence coming from colloidal glass model systems and computer simulations[17–19]. Nevertheless, it is not clear if such collective deformation through STZs is only present at temperatures below $T_g$ or also in the so-called supercooled liquid region where imprinting is carried out.

Building on our 2010 work[20] where we produced ultrasmooth featureless surfaces with corrugations of ≈0.2 nm using mica as a template, this work establishes imprinting of atomic-scale features with a similar ease as presently on the nano-length or micron-length scales. All details of complex atomically defined surface structures, as they were exhibited by strontium titanate (STO) single crystals, have been reproduced using $Pt_{57.5}Cu_{14.7}Ni_{5.3}P_{22.5}$, a BMG alloy shown to have high ductility, plasticity, and working time[8,21]. As the moulding process is similar to other highly scalable and practical nanomoulding methods but yields feature sizes dramatically smaller than these, we expect rapid proliferation of this finding and method (i) to study structure and deformation of glasses and (ii) for technological applications similar to those currently occupied by nanoimprinting, such as higher data density[1], larger surface areas in catalysts[5,10,11], or the precise shaping of surface morphologies for surface functionalization[4–6].

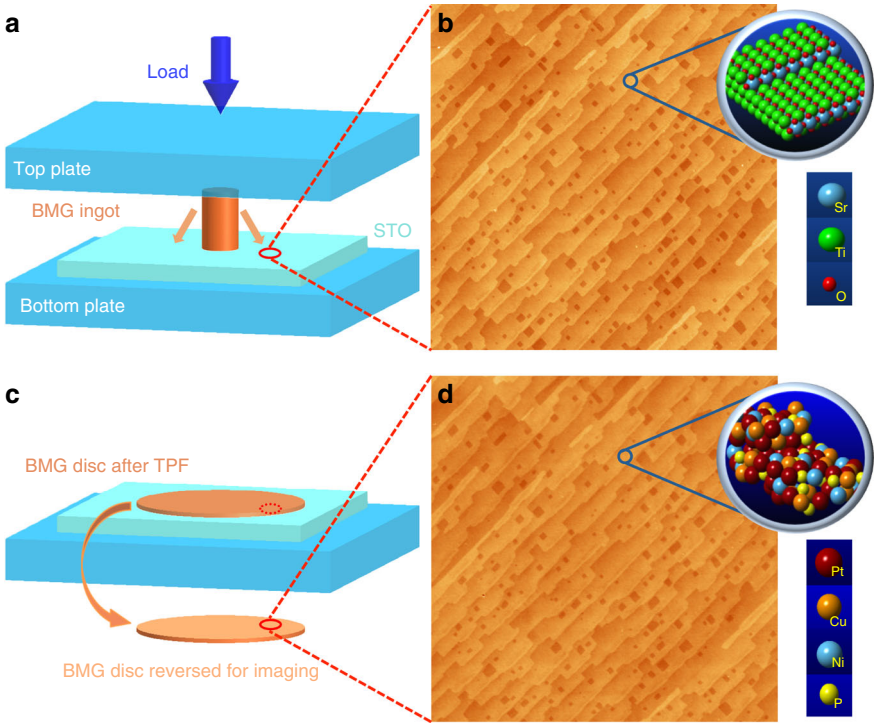


**Fig. 1** Thermoplastic imprinting with atomic precision. **a** Schematic representation of the geometric arrangement of the press used for the hot embossing, where a cylindrical ingot of bulk metallic glass (BMG) about 2.5 mm height and 2 mm in diameter is placed on the surface of a strontium titanate (STO) single crystal that has been prepared to feature individual atomically flat terraces separated by steps of unit cell (0.39 nm) height[22]. **b** Atomic force microscopy (AFM) image of the surface of an STO crystal used as a mould, revealing the aforementioned terraced surface structure. Inset: Structural model of the crystal's titanium dioxide ($TiO_2$) terminated, stepped (001) planes. **c** After imprinting is complete, the upper plate is removed and the formed BMG disc is separated from the STO template and turned over for AFM inspection. **d** Mirrored and *z*-inverted AFM image of the exact location that has been shaped by contact with the area of the STO crystal displayed in (**a**). Comparison with the template's original morphology shows that all details of the structure are reproduced with sub-ångstrom precision. Image size is in both cases 5 μm × 5 μm. The cartoon in the magnifier highlights the disordered (i.e. glassy) structure of the $Pt_{57.5}Cu_{14.7}Ni_{5.3}P_{22.5}$ alloy used for replication

## Results

**Thermoplastic imprinting with atomic precision**. A schematic of the imprinting (hot embossing) set-up is presented in Fig. 1a. With details of the imprinting method provided in the methods section below, the general procedure is as follows: first, the top plate as well as the bottom plate with the freshly prepared STO crystal placed onto it are heated at 270 °C, which was found to be the temperature Pt-BMG possesses the perfect viscosity for accurate flow. In the next steps, a BMG ingot is placed on the substrate and given time to equilibrate before the force is slowly ramped up to ≈1 kN. After holding that force for approximately three minutes, the force is relieved and the pressed sample is quickly cooled to room temperature by placing it on a large piece of copper and reversed for imaging (Fig. 1c).

A comparison between the corresponding locations of the original STO mould surface and the one of the BMG replica after imprinting is then shown in the Fig. 1b, d. Evaluating the similarities of the surface morphologies seen in the atomic force microscopy (AFM) images, we find that despite the small features —STO exhibits terraces as small as 100 nm in width and numerous mostly squared pits of unit cell (~0.39 nm) depth—all structural details of the STO template were accurately transferred into the BMG replica, thereby demonstrating atomically precise imprinting. This is particularly remarkable as the morphology observed on the STO mould results from energy minimization that favours the formation of atomically flat, $TiO_2$-terminated surfaces aligned with the crystal's (001) planes (magnifier in Fig. 1b)[22], while the BMG replica boasts a glassy structure, as illustrated by the cartoon in Fig. 1d showing a step edge replicated by disordered Pt, Cu, Ni and P atoms.

The findings of Fig. 1 suggest that the Pt-BMG flows in a viscous but liquid-like state, which, combined with favourable wetting properties, allows it to perfectly conform under pressure with the template's morphology before its shape is frozen in when the BMG is cooled below $T_g$. This hypothesis is corroborated by height profiles and surface roughness analyses performed on numerous BMG replicas that display the same step heights (0.39 nm) and terrace flatness as on the STO single crystal moulds (Fig. 2). For further characterization, X-ray diffraction, differential scanning calorimetry, and X-ray photoelectron spectroscopy measurements were performed on nanoimprinted BMG samples (see Supplementary Fig. 1). The results confirm that (i) imprinted samples are fully amorphous (Supplementary Fig. 1a), (ii) both imprinted BMG samples and as-cast BMG (i.e. before imprinting) have the same glass transition temperature, which agrees well with the literature value of 235 °C[23] (Supplementary Fig. 1b), and (iii) while some surface contamination due to air exposure is found (surface oxidation as well as some residual carbon; Supplementary Fig. 1c), no Ti or Sr is detected, indicating that material transfer from the mould to the replica is negligible.

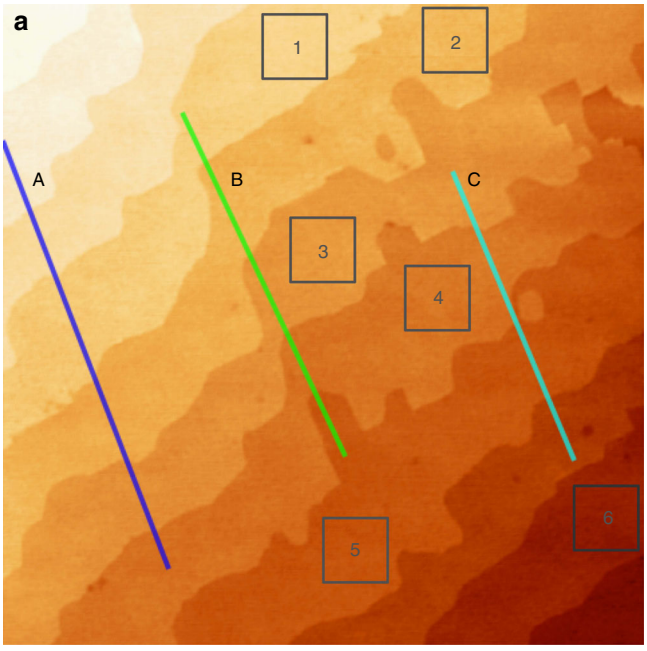


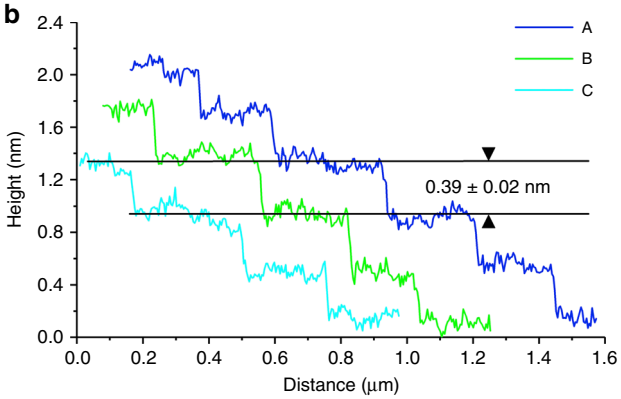


Roughness (RMS) on different terraces

| Position | 1 | 2 | 3 | 4 | 5 | 6 | Average |
|---|---|---|---|---|---|---|---|
| RMS (nm) | 0.056 | 0.061 | 0.053 | 0.060 | 0.059 | 0.069 | 0.060 ± 0.005 |

**Fig. 2** Roughness and height profiles analyses on a thermoplastically structured sample. **a** Representative atomic force microscopy image of an imprinted bulk metallic glass surface made from $Pt_{57.5}Cu_{14.7}Ni_{5.3}P_{22.5}$; image size: 2 μm × 2 μm. **b** Height profiles of the lines labelled in (**a**) with A, B and C and root mean square (RMS) roughness table of the areas 1–6, which are each 200 nm × 200 nm in size. The value found for the average roughness of 0.060 nm ± 0.005 nm matches well with the typical roughness of freshly prepared strontium titanate (STO) crystals. Combining all data, we recognize that despite its glassy nature, the replica exhibits atomically flat terraces with step heights of 0.39 nm ± 0.02 nm between them, which reflect the step height found on the STO moulds (STO crystallizes in a cubic perovskite structure with 0.3905 nm lattice parameter)

**Replica quality and reproducibility**. To examine reproducibility and the effect of loading time on replica quality, an STO crystal was used repeatedly; the AFM image in Fig. 3a shows an exemplary location on this crystal, but mirrored and with inverted $z$ scale to allow easy comparison with the imprints. Figure 3b–d then depicts images recorded on the equivalent location on three different replicas, which have been thermoplastically formed varying the time to ramp up the force the plates exert on the ingot from 0 N to 1 kN (loading time) from initially 1 min (Fig. 3b) to 2 min (Fig. 3c) and finally to 3 min (Fig. 3d), respectively. No apparent damage was observed on the STO surface even after employing it for three distinct experimental runs, thereby proving that moulds can be re-used without degradation, which again implies that there is no noticeable mass transport between templates and replicas. However, it can easily be seen that the run with 1 min loading time led to imperfect reproduction, as the AFM image of Fig. 3b exposes rough terraces.

To quantitatively assess the quality of replica formation, we calculated the surface roughness of all replicas as well as of the original STO crystal within the surface area highlighted by the squares in Fig. 3a–d. The results show that the roughness of the

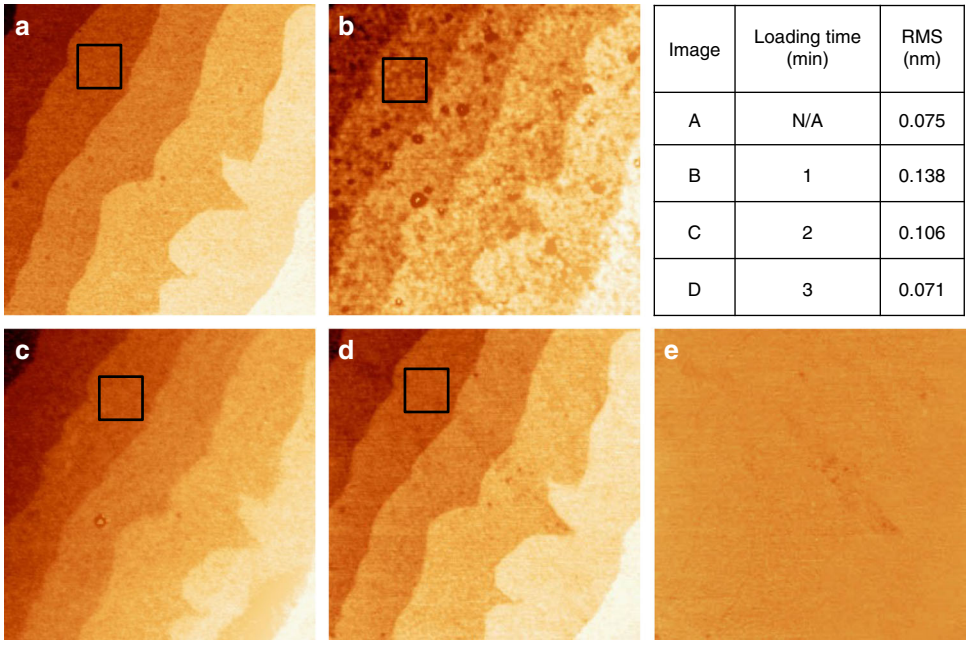


| Image | Loading time (min) | RMS (nm) |
|---|---|---|
| A | N/A | 0.075 |
| B | 1 | 0.138 |
| C | 2 | 0.106 |
| D | 3 | 0.071 |

**Fig. 3** Reproducibility and fidelity analysis. Atomic force microscopy images of **a** strontium titanate after having been used to press a total of four samples, mirrored and reversed for easy comparison with the imprints, and **b**–**d** bulk metallic glass replica of the surface area shown in (**a**), made from a $Pt_{57.5}Cu_{14.7}Ni_{5.3}P_{22.5}$ alloy and thermoplastically formed with loading times of **b** 1 min, **c** 2 min and **d** 3 min. To directly assess the quality of the replication, the table lists the root mean square (RMS) surface roughness values obtained from the corresponding areas marked by black squares. The side length of the squares of ≈250 nm was chosen to make best use of the terrace width on this sample. The image in **e** presents a merged image obtained by subtracting (**a**) from (**d**). All images are 2 μm × 2 μm

replica with 3 min loading time was virtually identical to that of the STO mould (Fig. 3a, d), while the surfaces of the replicas Fig. 3b, c were rougher, indicating that slower loading leads to better results. Loading times greater than 3 min, however, led again to a poor imprint quality because for such low loading rates, the BMG flows too fast when exposed to the plate's external force, which hinders pressure build-up and ultimately prevents reaching the optimum imprinting pressure of ≈10 MPa at the STO/BMG interface. On the other hand, loading times shorter than 1 min resulted frequently in a breakage of the STO substrate; we tentatively explain this outcome with an inability of the BMG to deform sufficiently at this time scale, which leads upon plate movement to a build-up of pressure that surpasses the substrate's breakage point. This points to time-dependent flow with fully homogeneous flow established during the slower loading, which allows the BMG to perfectly conform with the interface, while at shorter loading times, the BMG is unable to respond through a homogenous deformation but rather localized zones, which results in a more localized flow. Such localized flow may occur through shear-transformation events, which have been suggested as flow units in metallic glasses[15,24–26].

**Replica fidelity and long-term stability**. Another way to assess the fidelity of feature replication is presented in Fig. 3e, which shows data obtained by subtracting the image Fig. 3a from the one in Fig. 3d. Since perfect reproduction would result in a flat plane, any visible contrast conveniently identifies imperfections in the replication fidelity. With Fig. 3e being almost entirely uniform, we have further confirmation of the high quality of the atomic-scale replication. The few diffuse features visible are likely due to post-imprint contamination and/or surface oxidation occurring under ambient conditions on both the STO substrate and the BMG replica rather than due to an imperfect imprinting process. Finally, to determine the stability of the imprinted structures, we re-imaged the BMG replica shown in Fig. 3d, 32 months after thermoplastic forming without performing any surface cleaning. As seen in Fig. 4, the ~1000 days of air exposure did not noticeable degrade the structure, indicating that imprinted BMG surfaces are very stable. For comparison, atomic structures on the surface of STO degrade visibly within days to weeks after annealing.

## Discussion

This work establishes the feasibility of creating high-fidelity replica of atomic-sized features from BMGs that are both reproducible and stable through an easy-to-implement, low-cost process. These are distinctive advantages compared to work by Yoshimoto et al., who were able to stamp a pattern arising from straight, evenly spaced steps produced by sapphire crystals into silicate glass[27–29] and poly(methyl methacrylate) (PMMA)[29], but whose replicas lacked replication of complex, small-scale patterns. In addition, the silicate glass had to be processed at rather high temperatures (>580 °C), while polymers showed an ≈1/3 increase in roughness and ≈1/3 decrease in the measured step heights compared to the sapphire mould, which was assigned to thermal shrinkage and viscoelastic relaxation of the polymer macromolecules[29]. Generating atomically smooth glass surfaces also has the potential to unveil the structural arrangement and local distribution of individual chemical species in amorphous materials, thereby promoting unprecedented insight into the nature of the glassy/liquid state. Technologically, the ability to manipulate BMGs on the atomic scale opens up possibilities to maximize the surface area of metals to its theoretical limit, a long-sought-after goal in a wide range of surface dominated applications including sensors, catalysts, and batteries.

## Methods

**Preparation of the STO (100) moulds**. $TiO_2$-terminated STO (100) crystals with one side polished were purchased from CrysTec GmbH (Berlin, Germany) and

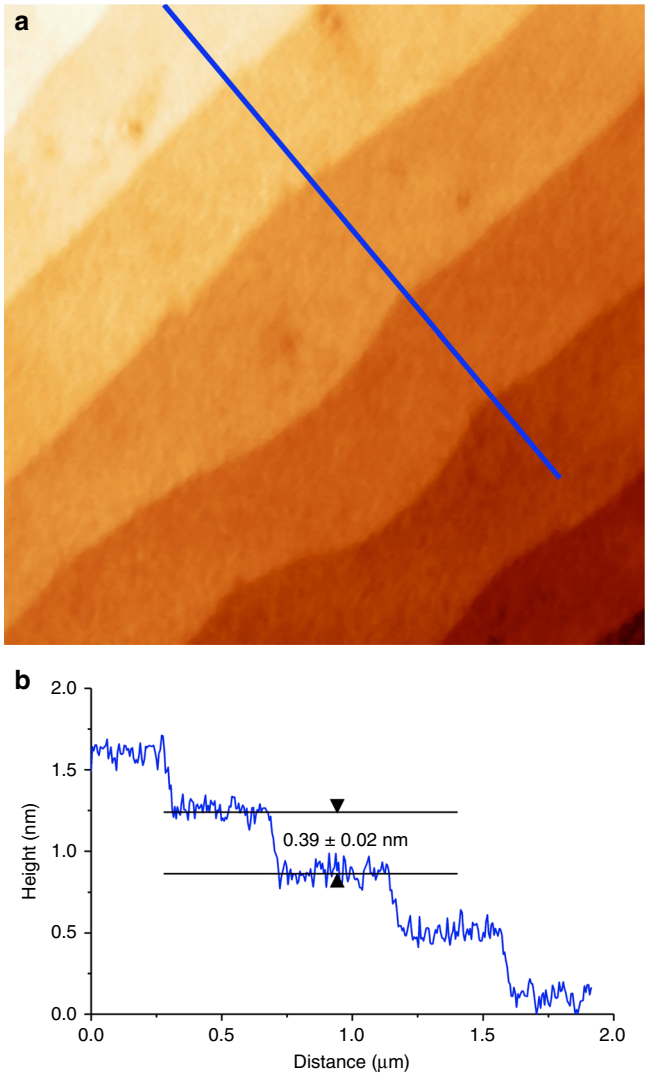


**Fig. 4** Assessment of the long-term stability of imprinted BMG samples. **a** Atomic force microscopy image taken on an imprinted $Pt_{57.5}Cu_{14.7}Ni_{5.3}P_{22.5}$ bulk metallic glass after having been stored in ambient conditions for 32 months after forming; image size is 2 μm × 2 μm. Despite the long time that passed, steps and terraces appear with the same clarity as they did immediately after preparation. More specifically, we found that the average root mean square surface roughness on the terraces increased only modestly from 0.071 nm immediately after preparation to ≈0.085 nm, an effect that is likely due to increased surface oxidation and the absorption of contaminants from the air. **b** Height profile along the line in (**a**), exhibiting the steps heights that correspond again well with the strontium titanate lattice parameter of 0.3905 nm

MTI Corporation (Richmond, CA, USA). Atomically flat surface terminations with structures as shown in Figs. 1a, 3a were then obtained by rinsing the as-polished surfaces three times with both acetone and distilled water to remove contaminants followed by ultrasonic agitation in distilled water (10 min) and annealing in air (1000 °C for 2 h)[30].

**Atomic-scale imprinting by thermoplastic forming**. Custom heating plates were installed on a load cell of an Instron 5569 mechanical testing machine to allow a precise control of temperature at 270 °C ± 0.5 °C and applied pressure during moulding experiments. A schematic of the imprinting set-up is shown in Fig. 1a. Once the temperature of the plates and of an STO crystal placed on the lower plate and prepared as described above had reached a steady state, an ingot of $Pt_{57.5}Cu_{14.7}Ni_{5.3}P_{22.5}$ (Pt-BMG) with ≈2.5 mm height and ≈2 mm diameter is placed on the surface of an STO single crystal that has been prepared as described above to exhibit a clean surface structure of atomically flat terraces separated by steps of unit cell (i.e. 0.39 nm) height; the right part of the panel shows an atomic force microscopy (AFM) image of the as-prepared STO surface. Thermoplastic forming is carried out by ramping the force exerted by the plates up to 1 kN (≈10 MPa) with both the top and bottom plates heated to 270 °C, which is in the BMG's supercooled liquid region bounded by its $T_g$ of ≈235 °C and its crystallization temperature $T_c$ ≈ 297 °C [8,21,23]. A processing temperature of 270 °C has been found as the best compromise between realizing a viscosity that is enabling adequate ease of imprinting and sufficient processing time before crystallization, with ~15 min processing window before crystallization occurs[12]. While the loading rate was varied, the maximum applied load of 1 kN was kept constant for 3 min after the loading ramp had been completed in all cases. After removal from the load cell, the samples were quickly cooled down in ambient condition by transferring them onto a large copper plate kept at room temperature. Since we were using cubic phase STO crystals as moulds, the differences in thermal expansion coefficients between the oxide substrate and the BMG replica combined with the fact that the inner cohesion of both materials is considerably stronger than the adhesion at the interface triggered the newly pressed BMG disc to separate from the mould during cooling by itself without loss of replica fidelity, exposing the clean surface for immediate further investigation by AFM (cf. Figure 1b). The image in the right part of panel b in Fig. 1 shows the location replicated by the area on the STO substrate shown in panel a, but mirrored and *z*-inverted to facilitate comparison.

**AFM characterization**. AFM characterization was carried out under ambient conditions in tapping mode, with the data of Fig. 3 being acquired by using a Bruker Dimension Fastscan AFM equipped with a PPP-NCL-50 silicon cantilever from Nanosensors (Neuchâtel, Switzerland) that featured a driving frequency of 164 kHz. All other AFM images were obtained using a Bruker Multimode AFM with Nanoscope III electronics and Bruker RTESPAW-300 silicon cantilevers with driving frequencies ranging from 290 to 300 kHz. As described in Fig. 4, imprinted BMG surfaces were found to be very stable and could be re-imaged for months following preparation without any apparent loss of resolution. To facilitate the comparison of the surface morphologies of mould and replica, the original AFM image of either the as-imprinted Pt-BMG (Fig. 1b) or the STO substrate (Fig. 3a) were mirrored along the *y*–*z* plane-followed by inverting the image's *z*-scale using data processing software. After completing such symmetry operation, the patterns observed for a perfectly imprinted replica should be identical to that of the original mould.

## Data availability

The data that support the results within this paper and other findings of this study are available from the corresponding author on reasonable request.

Received: 6 September 2018 Accepted: 11 October 2018
Published online: 05 November 2018

## References

1. Chou, S. Y., Krauss, P. R. & Renstrom, P. J. Imprint lithography with 25-nanometer resolution. *Science* **272**, 85–87 (1996).
2. Hua, F. et al. Polymer imprint lithography with molecular-scale resolution. *Nano Lett.* **4**, 2467–2471 (2004).
3. Gates, B. D. et al. New approaches to nanofabrication: molding, printing, and other techniques. *Chem. Rev.* **105**, 1171–1196 (2005).
4. Li, Z. et al. Hybrid nanoimprint-soft lithography with sub-15 nm resolution. *Nano Lett.* **9**, 2306–2310 (2009).
5. Hernandez, J. J. et al. Multifunctional nano-engineered polymer surfaces with enhanced mechanical resistance and superhydrophobicity. *Sci. Rep.-Uk* **7**, 43450 (2017).
6. Zhou, W. *Nanoimprint Lithography: An Enabling Process for Nanofabrication*. (Springer, Heidelberg 2013).
7. Johnson, W. L. Bulk glass-forming metallic alloys: science and technology. *MRS Bull.* **24**, 42–56 (1999).
8. Schroers, J. & Johnson, W. L. Highly processable bulk metallic glass-forming alloys in the Pt–Co–Ni–Cu–P system. *Appl. Phys. Lett.* **84**, 3666–3668 (2004).
9. Schroers, J. Processing of bulk metallic glass. *Adv. Mater.* **22**, 1566–1597 (2010).
10. Cui, Z. *Nanofabrication*. 2 edn, (Springer International Publishing, Switzerland 2017).
11. Saito, T. & Ito, H. in *Nanoimprint Technology* 17-50 (John Wiley & Sons, Ltd, eds. Jan Taniguchi, Hiroshi Ito, Jun Mizuno & Taushi Saito. Chichester, West Sussex, UK 2013).
12. Kumar, G., Tang, H. X. & Schroers, J. Nanomoulding with amorphous metals. *Nature* **457**, 868–872 (2009).

13. Kumar, G., Desai, A. & Schroers, J. Bulk metallic glass: the smaller the better. *Adv. Mater.* **23**, 461–476 (2011).
14. Chiu, H. M., Kumar, G., Blawzdziewicz, J. & Schroers, J. Thermoplastic extrusion of bulk metallic glass. *Scr. Mater.* **61**, 28–31 (2009).
15. Argon, A. S. Plastic-deformation in metallic glasses. *Acta Metall. Mater.* **27**, 47–58 (1979).
16. Greer, A. L., Cheng, Y. Q. & Ma, E. Shear bands in metallic glasses. *Mat. Sci. Eng. R* **74**, 71–132 (2013).
17. Falk, M. L. & Langer, J. S. Dynamics of viscoplastic deformation in amorphous solids. *Phys. Rev. E* **57**, 7192–7205 (1998).
18. Hufnagel, T. C., Schuh, C. A. & Falk, M. L. Deformation of metallic glasses: recent developments in theory, simulations, and experiments. *Acta Mater.* **109**, 375–393 (2016).
19. Schuh, C. A. & Lund, A. C. Atomistic basis for the plastic yield criterion of metallic glass. *Nat. Mater.* **2**, 449–452 (2003).
20. Kumar, G., Staffier, P. A., Blawzdziewicz, J., Schwarz, U. D. & Schroers, J. Atomically smooth surfaces through thermoplastic forming of metallic glass. *Appl. Phys. Lett.* **97**, 101907 (2010).
21. Schroers, J. & Johnson, W. L. Ductile bulk metallic glass. *Phys. Rev. Lett.* **93**, 255506 (2004).
22. Kawasaki, M. et al. Atomic Control of the $SrTiO_3$ Crystal. *Surf. Sci.* **266**, 1540–1542 (1994).
23. Schroers, J. On the formability of bulk metallic glass in its supercooled liquid state. *Acta Mater.* **56**, 471–478 (2008).
24. Schall, P., Weitz, D. A. & Spaepen, F. Structural rearrangements that govern flow in colloidal glasses. *Science* **318**, 1895–1899 (2007).
25. Langer, J. S. Dynamics of shear-transformation zones in amorphous plasticity: formulation in terms of an effective disorder temperature. *Phys. Rev. E Stat. Nonlin. Soft Matter Phys.* **70**, 041502 (2004).
26. Langer, J. S. Shear-transformation-zone theory of plastic deformation near the glass transition. *Phys. Rev. E Stat. Nonlin. Soft Matter Phys.* **77**, 021502 (2008).
27. Miyake, Y. et al. Nanoimprint fabrication and thermal behavior of atomically ultrasmooth glass substrates with 0.2-nm-height steps. *Jpn J. Appl. Phys.* **50**, 078002 (2011).
28. Suga, O. et al. Atomic step patterning on quartz glass via thermal nanoimprinting. *Jpn. J. Appl. Phys.* **54**, 098001 (2015).
29. Yoshimoto, M. Sub-nanoscale nanoimprint fabrication of atomically stepped glassy substrates of silicate glass and acryl polymer. *Appl. Phys. a-Mater.* **121**, 321–326 (2015).
30. Woo, S. et al. Surface properties of atomically flat poly-crystalline SrTiO3. *Sci. Rep.-Uk* **5**, 8822 (2015).

## Acknowledgements

We thank the Department of Energy for funding through Grant No. DE-SC0016179. Initial work predating this grant was supported by the National Science Foundation through Grant No. MRSEC DMR-1119826.

## Author contributions

U.D.S. conceived and directed the work and R.L. and G.H.S. designed the experimental procedure. Experiments were conducted by R.L., Z.C., C.Z. and G.H.S. with support by A.D., J.K., E.K., Z.L., O.E.D., S.S., J.P.S., C.O.O. and, Z.C., A.D. R.L. and J.S. analysed the data and collaborated with U.D.S. to compose the manuscript. All authors discussed and commented on the manuscript.

## Additional information

**Supplementary information** accompanies this paper at https://doi.org/10.1038/s42005-018-0076-6.

**Competing interests:** The authors declare no competing interests.

**Reprints and permission** information is available online at http://npg.nature.com/reprintsandpermissions/

**Publisher's note:** Springer Nature remains neutral with regard to jurisdictional claims in published maps and institutional affiliations.